Fiber Distribution in UHPC Beams:

An Insight from 3D Micro-CT Scans on Shear Tests

d = 250 mm d = 10 in | d = 500 mm d = 20 in | d = 750 mm d = 30 in | d = 1000 mm d = 39 in

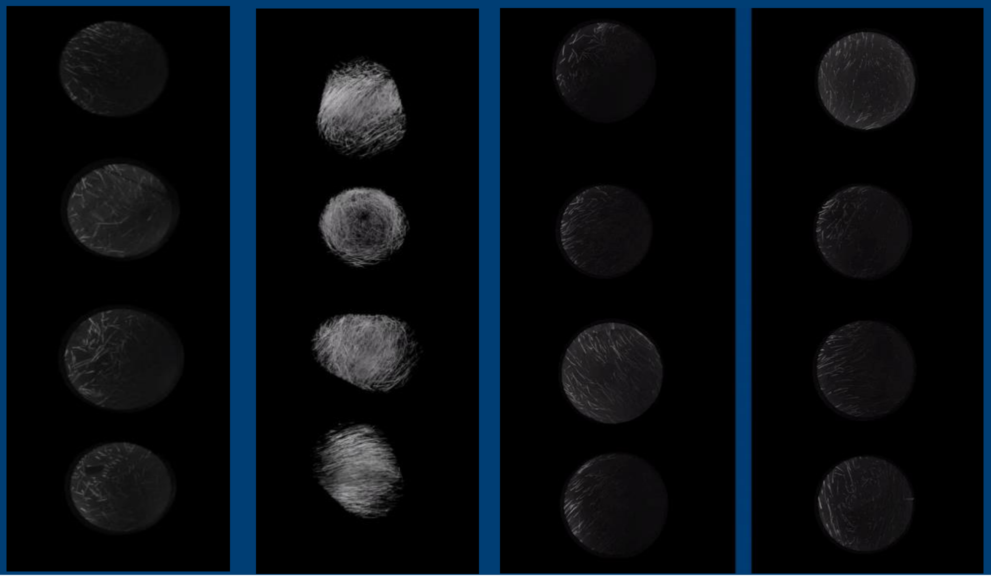

Manuel Bermudez Ph.D. Candidate
Chung-Chan Hung Professor

國立成功大學
National Cheng Kung University
1931

American Concrete Institute

APRIL 2-6, 2023
SAN FRANCISCO, CA, USA

Does the beams' depth impact the fiber distribution characteristics in UHPC beams?

For all beams

- Straight steel fiber: Length→ 13mm Diameter→ 0.2mm
- Casting at the end of the beam
- Longitudinal reinforcement ratio ρ = 3.4%
- 3-point load configuration

L = 1530 mm , h = 300 mm
L = 60 in , h = 12 in

d = 250 mm
d = 10 in

L = 4200 mm , h = 1150 mm
L = 165 in , h = 45 in

d = 1000 mm
d = 39 in

FBD of the forces acting at the inclined shear crack

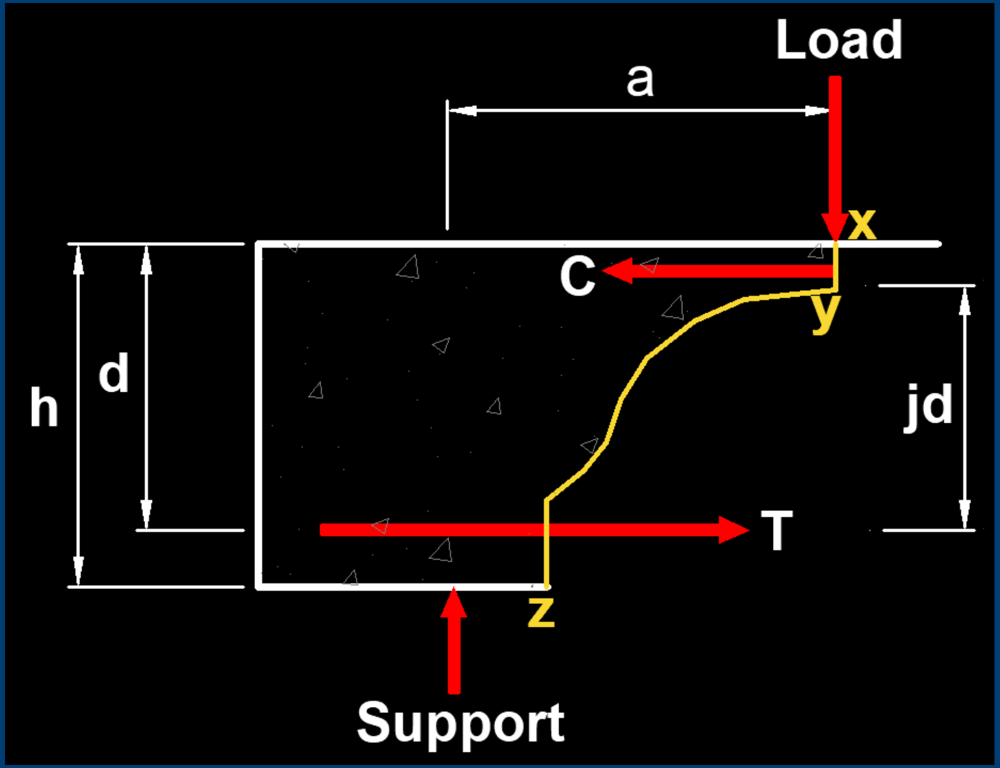

Location of the cores for the micro-CT

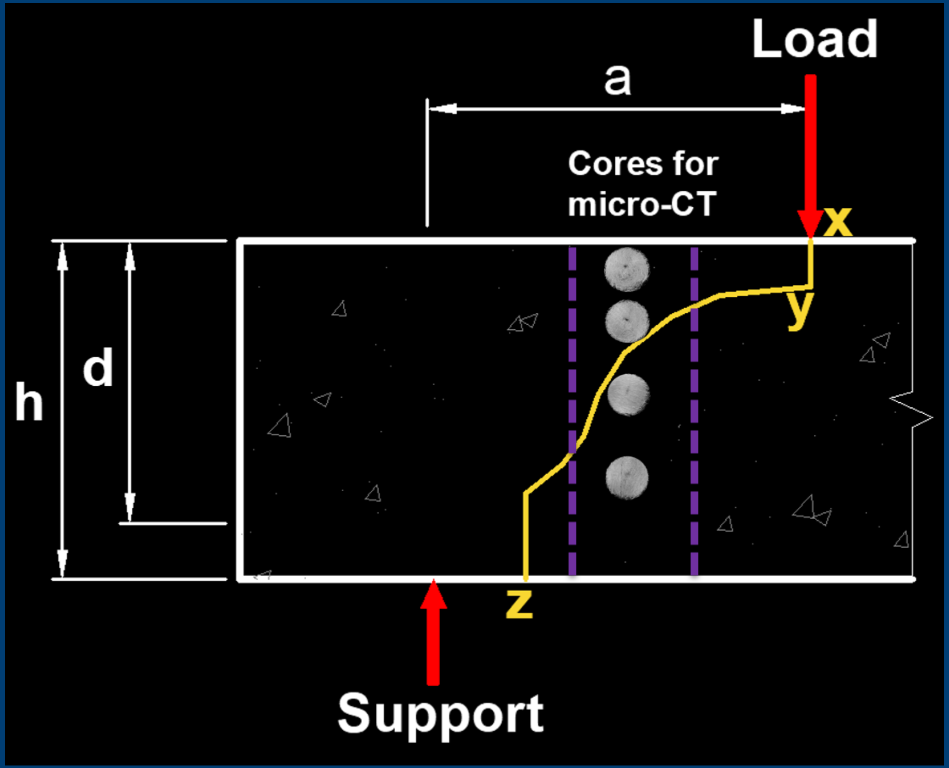

Notation

Line x-y-z = Inclined shear crack

a = shear span

d = effective depth

h = height

jd= internal moment arm

T = tension force

C = compression force

L = 3380 mm, h = 850 mm

L = 133 in , h = 33 in

Obtaining Drilled Cores from UHPC I-shaped beams

Core drilling on flanges

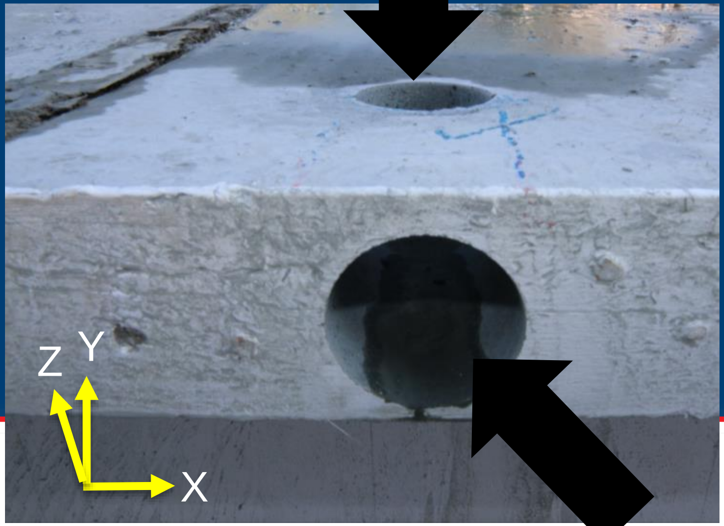

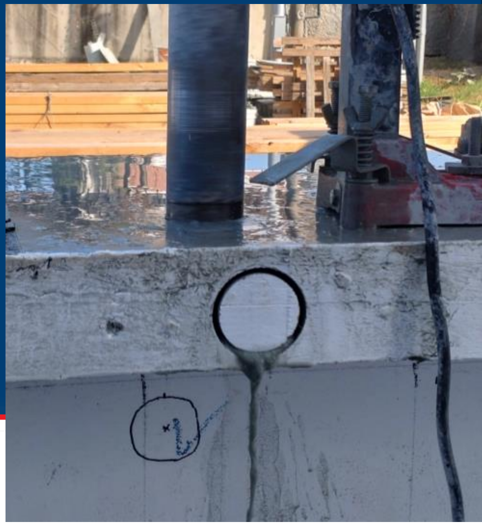

Issues with drilling cores in the longitudinal direction of the UHPC I-shaped beams



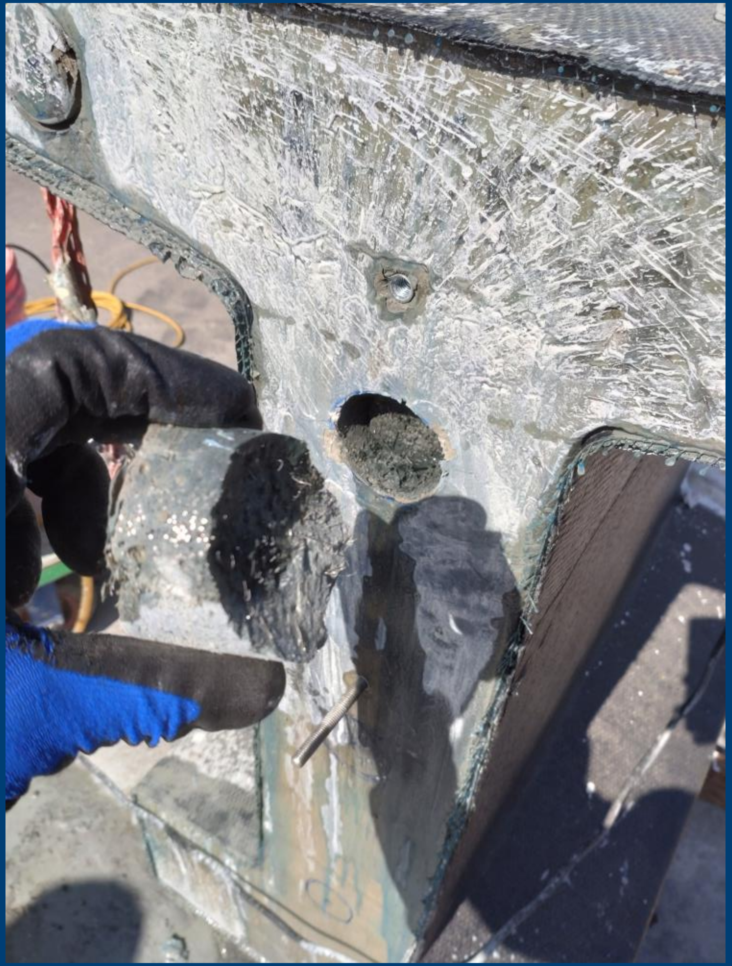

Easy to drill a ≥150 mm (6 in) long core

Impossible to extract the core due to the fibers in the core end

Preparing the UHPC core samples for the micro-CT scans

Step 1

55 mm (2 in)

≥150 mm (6 in)

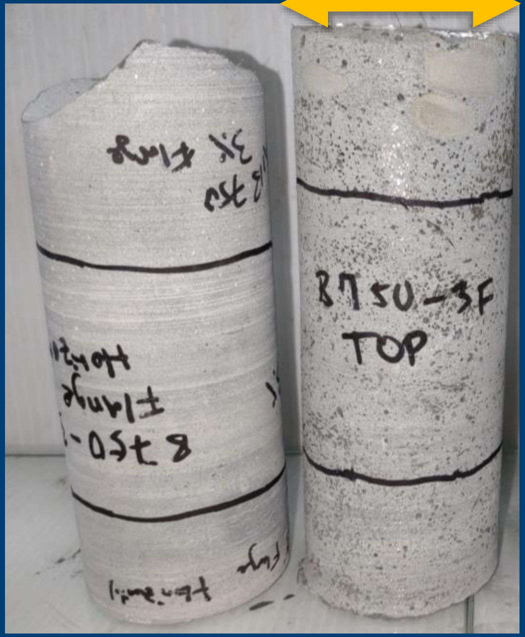

≥55 mm (2 in)

≥39 mm (1 in) =3L_f

If the 13-mm steel fibers of this core that had V_f of 1.5% were linearly aligned, the 1657 fibers would have a total length of 21.5 m (846 in).

Step 2

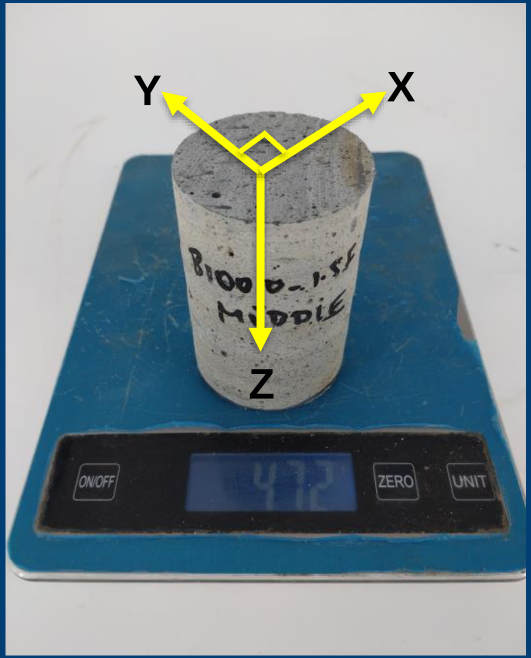

Step 3

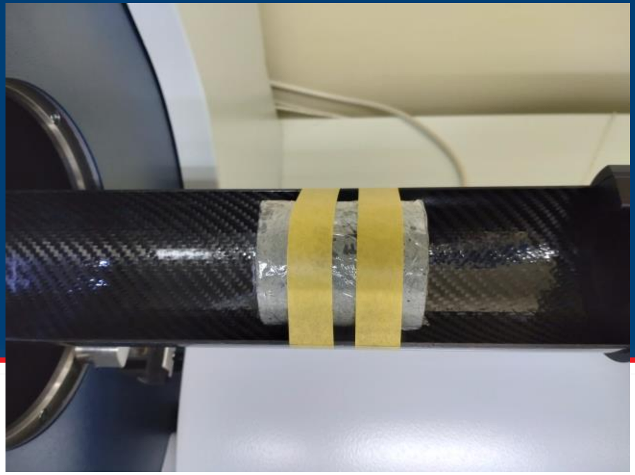

3D dimensional volume distribution of the micro-CT images

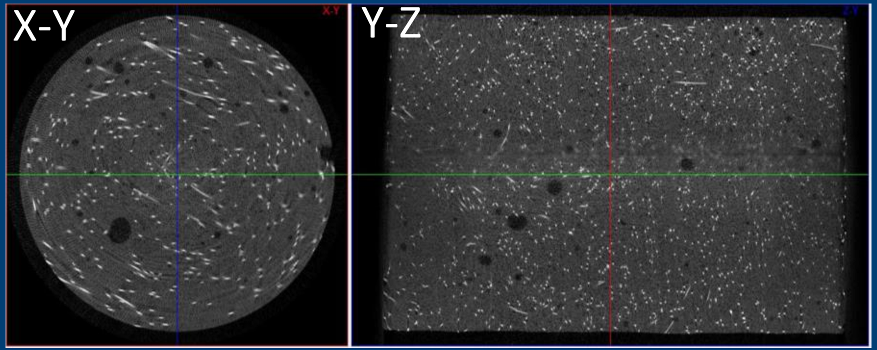

V_f =1.50%

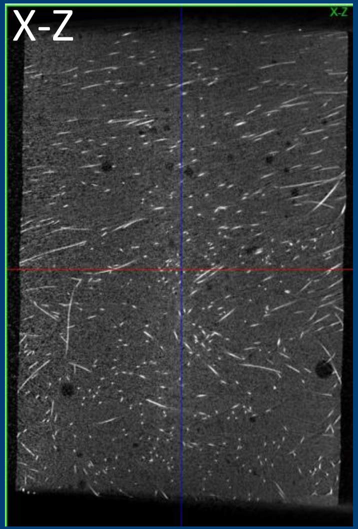

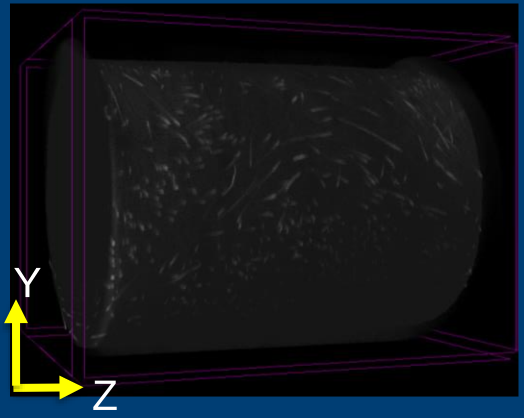

SKYSCAN 1276 micro-CT	
3D images with high-resolution	spiral (helical) fashion
Tube voltage	100 kV
Exposure time	0.205s
Filler material	Al and Cu

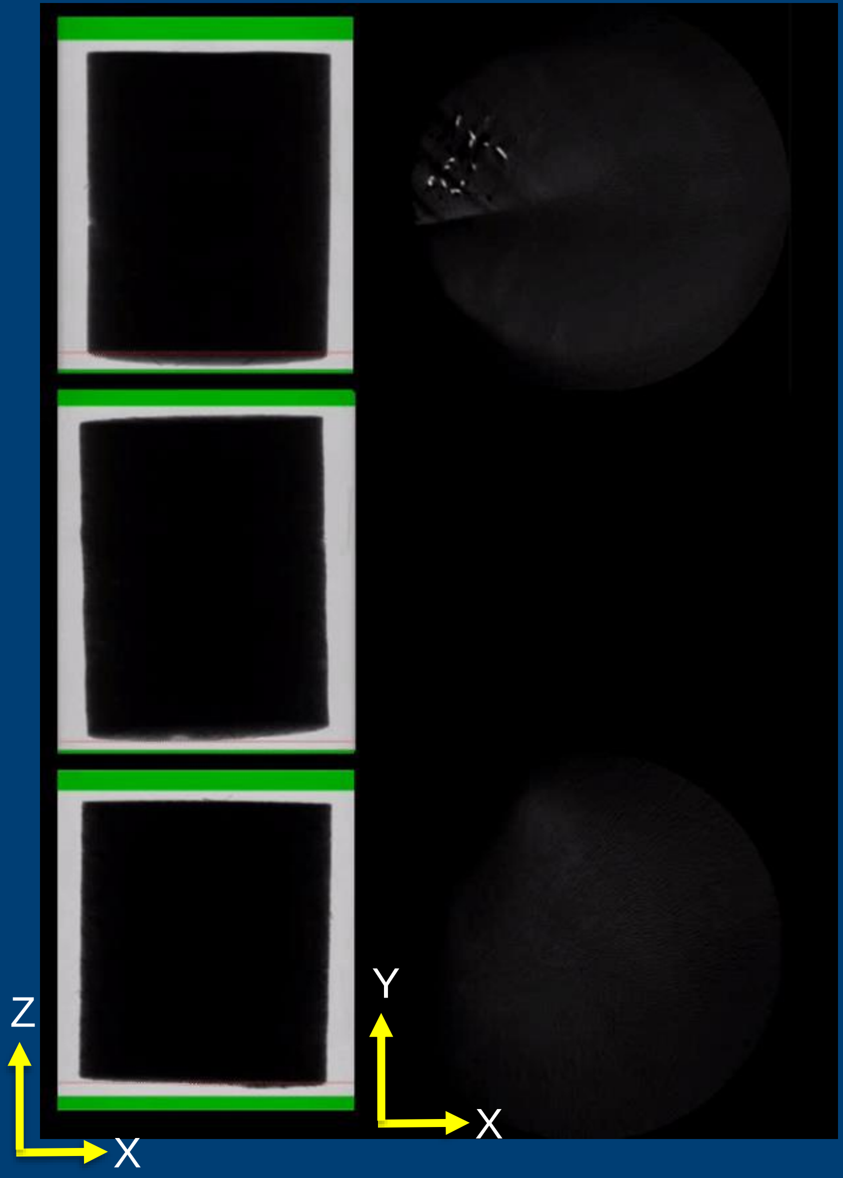

V_f =0.75%

V_f =1.50%

V_f =3.00%

2D images that are slices of the 3D volume

Qualitative analysis of fiber distribution on shear tests of UHPC beams

Shear tests for size effect assessment

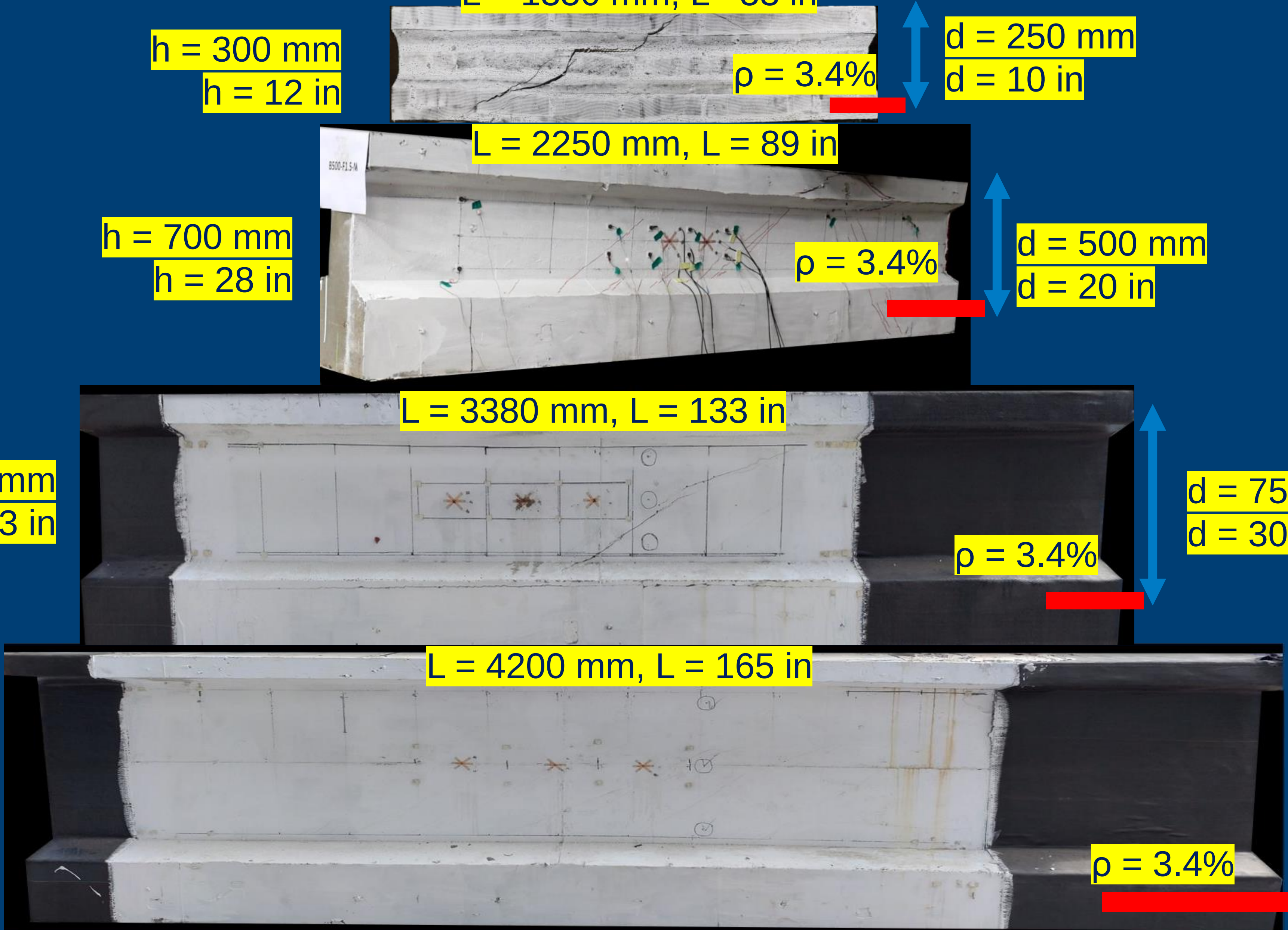

3D images of shear tests with increasing beams' depth

Cross-sectional view

d = 250 mm (10 in)

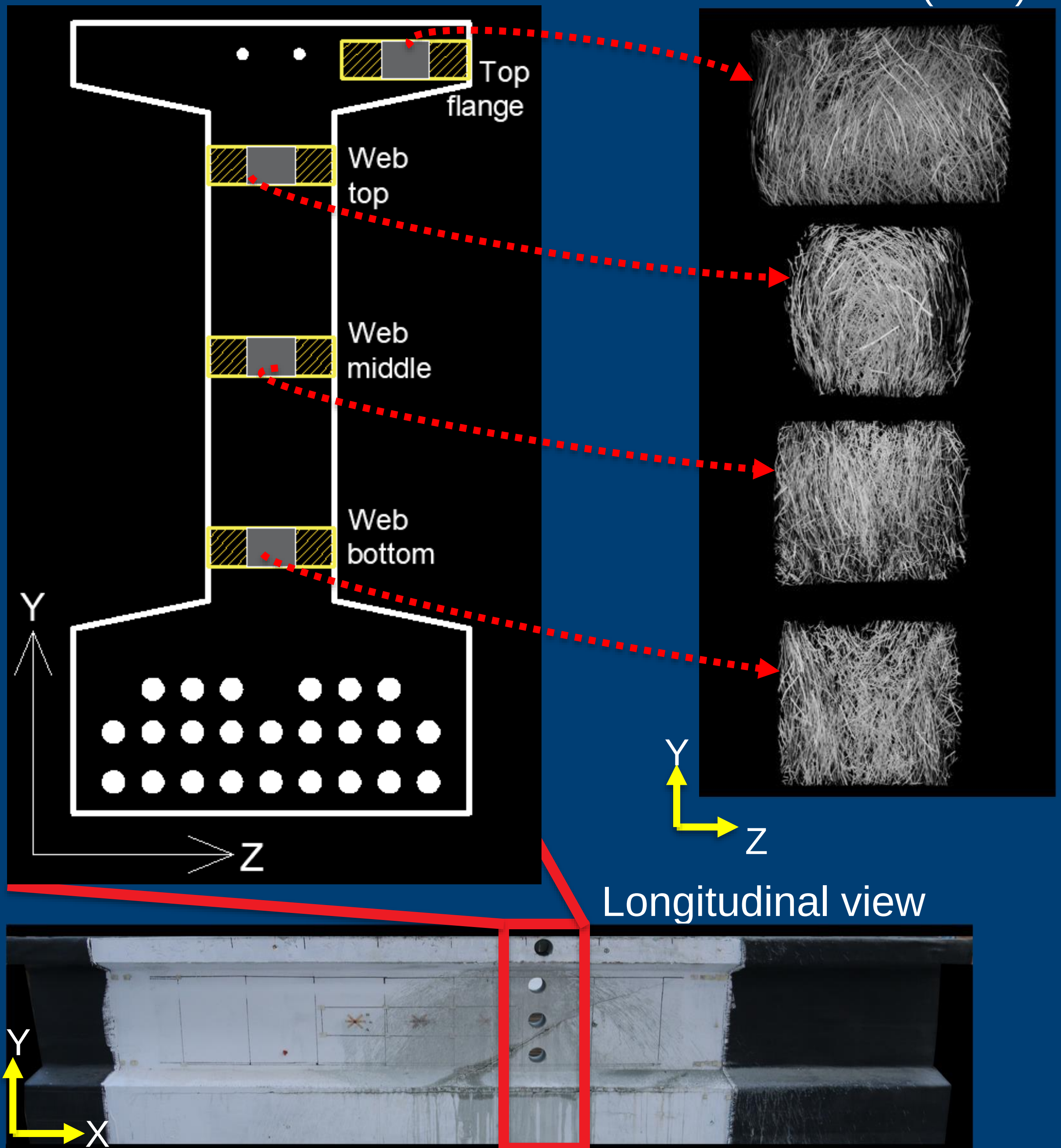

All beams with V_f =1.50%

3D images of shear tests with increasing beams' depth

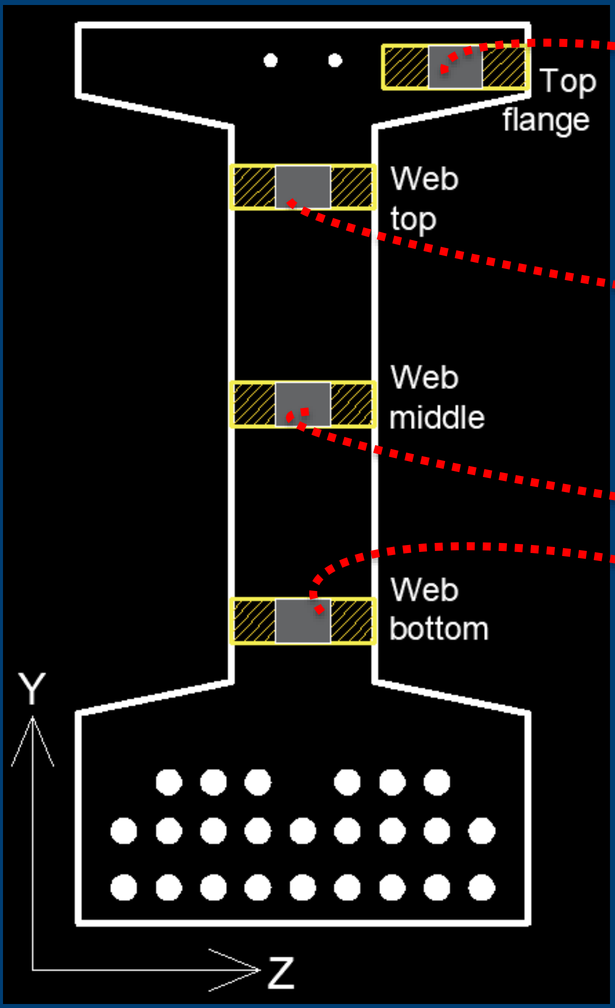

d = 250 mm (10 in) | d = 500 mm (20 in) | d = 750 mm (30 in) | d = 1000 mm (39 in)

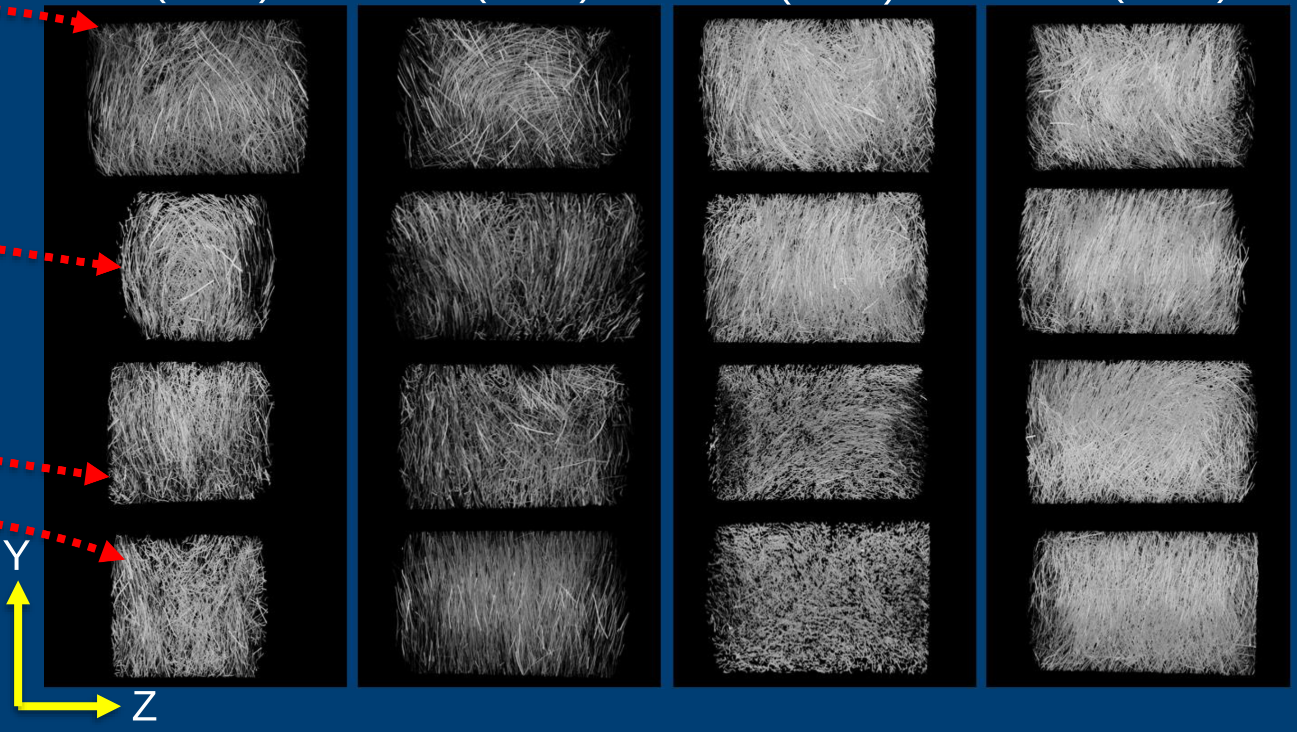

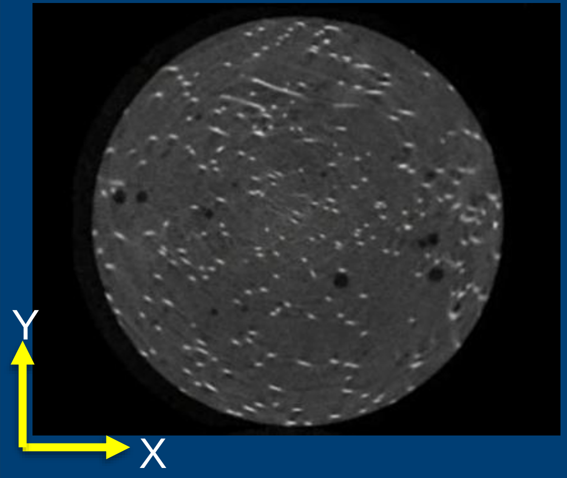

Beam's depth	d = 250 mm	d = 500 mm	d = 750 mm	d = 1000 mm
Location	**The inclination angle of the majority of the fibers in the X-Y Axis**			
Top flange	CAT.1 15° - 180°	CAT.1 15° - 180°	CAT.1 15° - 180°	CAT.1 15° - 180°
Web top	CAT.1 15° - 180°	CAT.1 15° - 180°	CAT.2 15° - 150°	CAT.2 15° - 150°
Web middle	CAT.1 15° - 180°	CAT.2 15° - 150°	CAT.4 0° - 15°	CAT.3 5° - 30°
Web bottom	CAT.2 15° - 150°	CAT.4 0° - 15°	CAT.4 0° - 15°	CAT.4 0° - 15°

Orientation Category	Range of Inclination Angles in the X-Y axis
1 Random	15° - 180°
2 Partially random	15° - 150°
3 Partially preferred	0° - 30°
4 Preferred	0° - 15°

Shear tests for fiber volume fraction assessment

L = 3380 mm, h = 850 mm
L = 133 in , h = 33 in

Vf = 0.75%

Vf = 1.50%

ρ = 3.4%

d = 750 mm
d = 30 in

3D images of shear tests different fiber volume fractions

Cross-sectional view

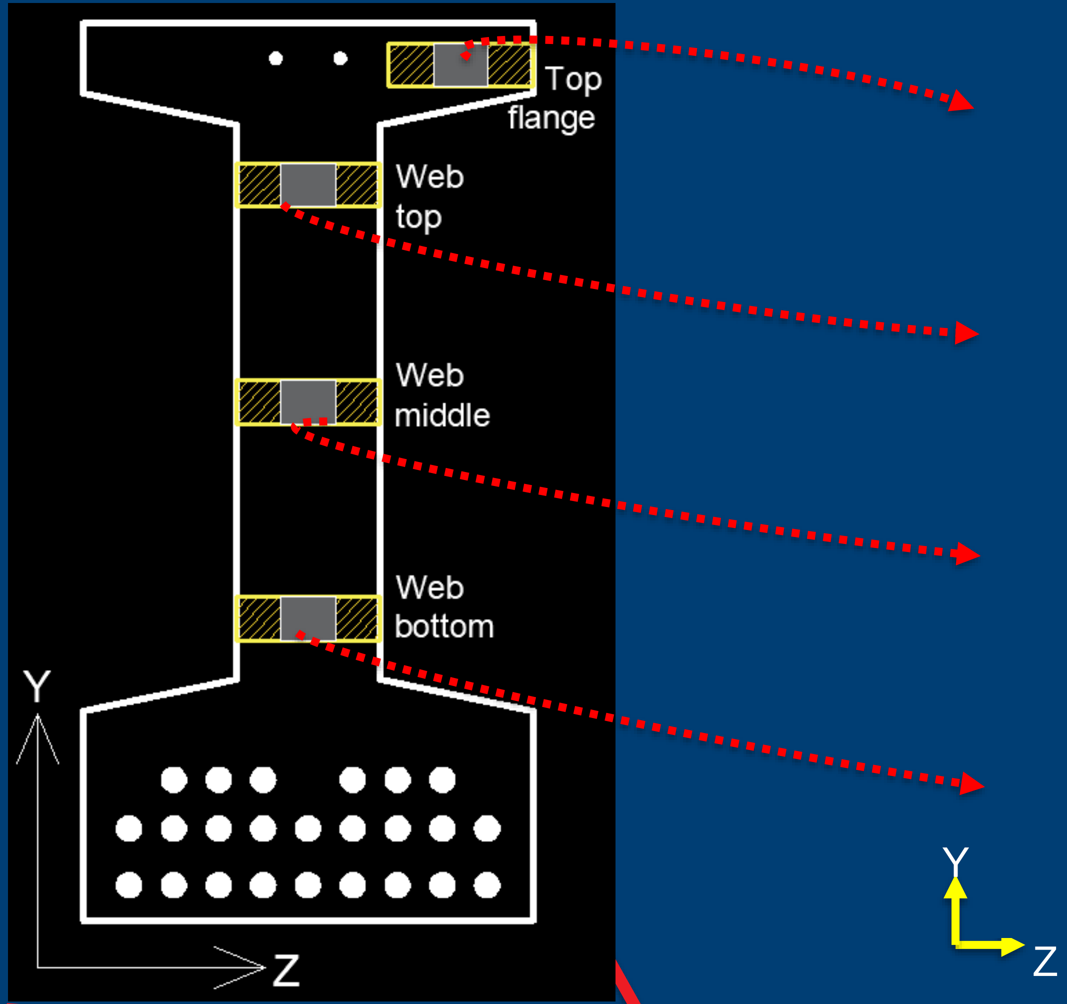

V_f = 1.50%

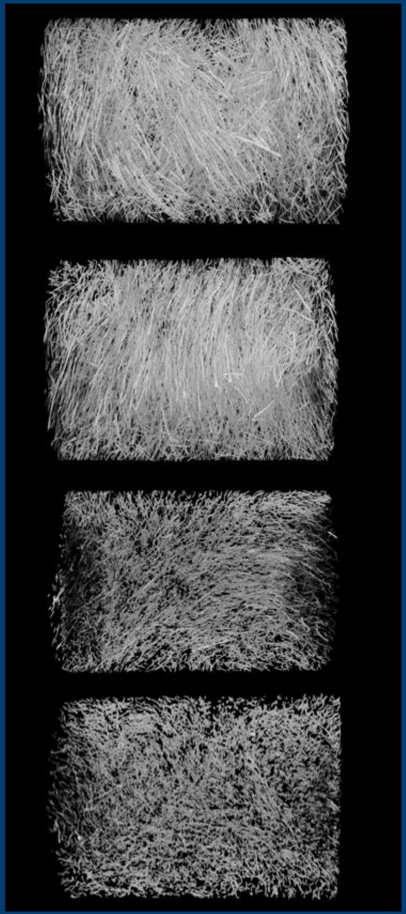

Longitudinal view

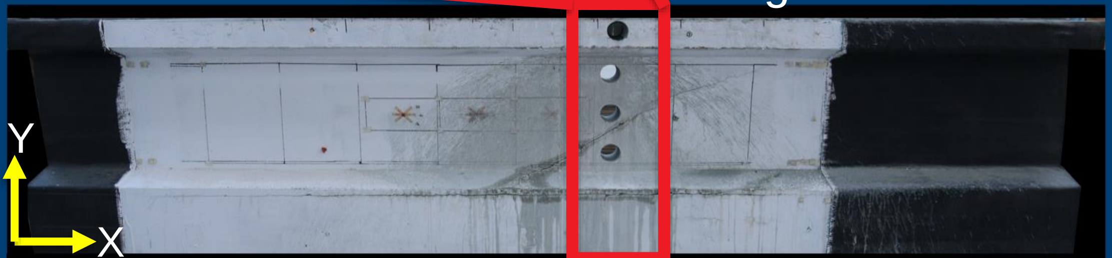

All beams with d = 750 mm (30 in),
L = 3380 mm (133 in), h = 850 mm (33 in)

3D images of shear tests with increasing beams' depth

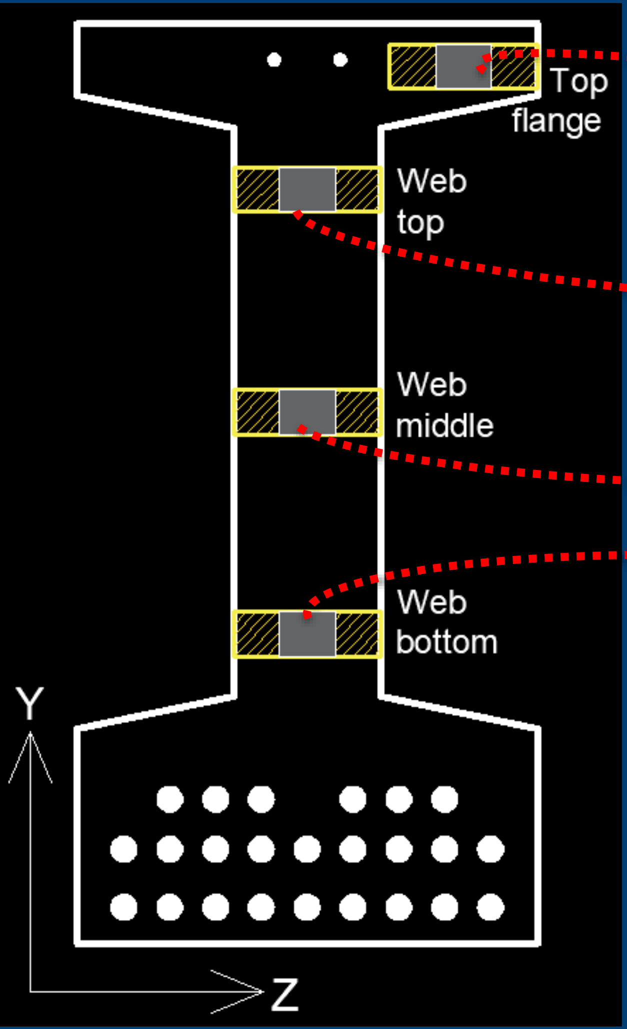

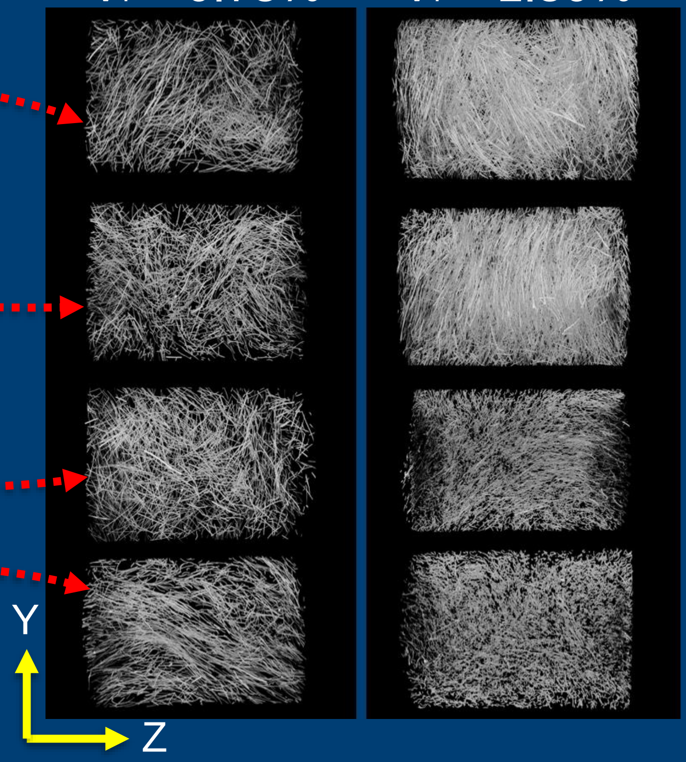

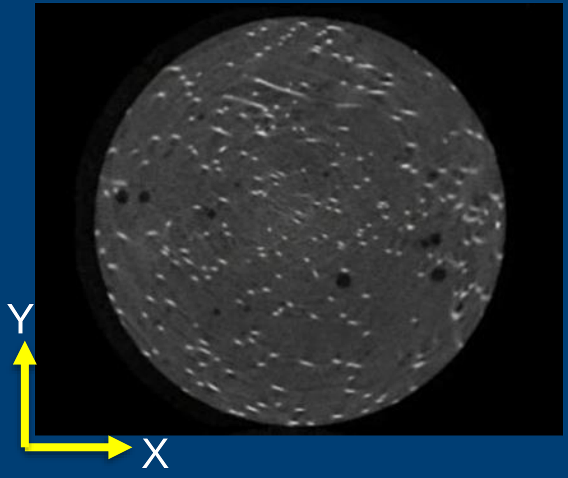

Beam's fiber volume fraction	V_f = 0.75%	V_f = 1.50%
Location	**The inclination angle of the majority of the fibers in the X-Y Axis**	
Top flange	CAT.1 15° - 180°	CAT.1 15° - 180°
Web top	CAT.1 15° - 180°	CAT.2 15° - 150°
Web middle	CAT.2 15° - 150°	CAT.4 0° - 15°
Web bottom	CAT.2 15° - 150°	CAT.4 0° - 15°

Orientation Category	Range of Inclination Angles in the X-Y axis
1 Random	15° - 180°
2 Partially random	15° - 150°
3 Partially preferred	5° - 30°
4 Preferred	0° - 15°

Implications of the fiber distribution on shear strength of UHPC beams

1 Fiber efficiency varies along the shear crack of UHPC beams

Beams with depths of 250 mm (10 in) have the same fiber efficiency along the shear crack

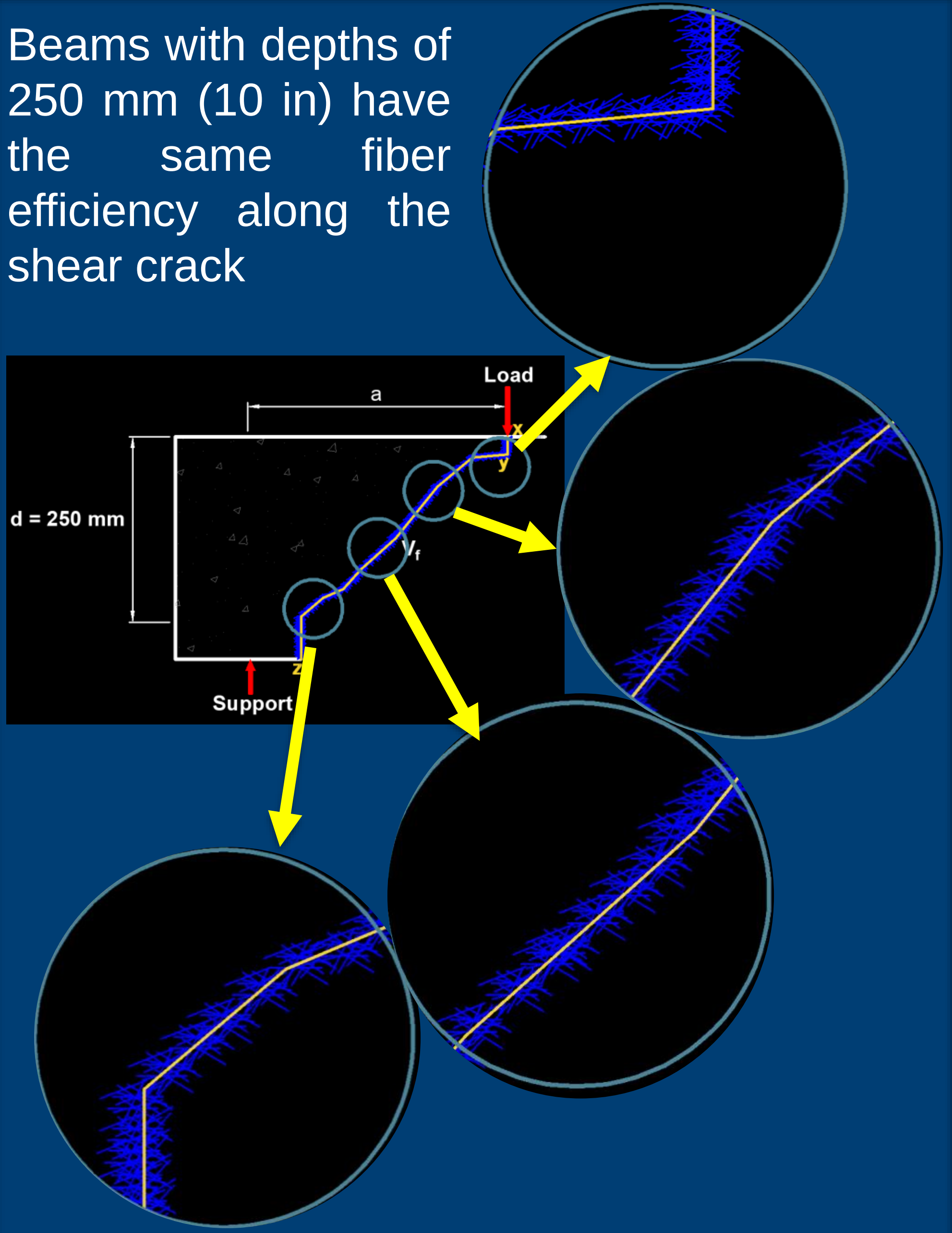

Beams with depths of 1000 mm (39 in) have varying fiber efficiency along the shear crack

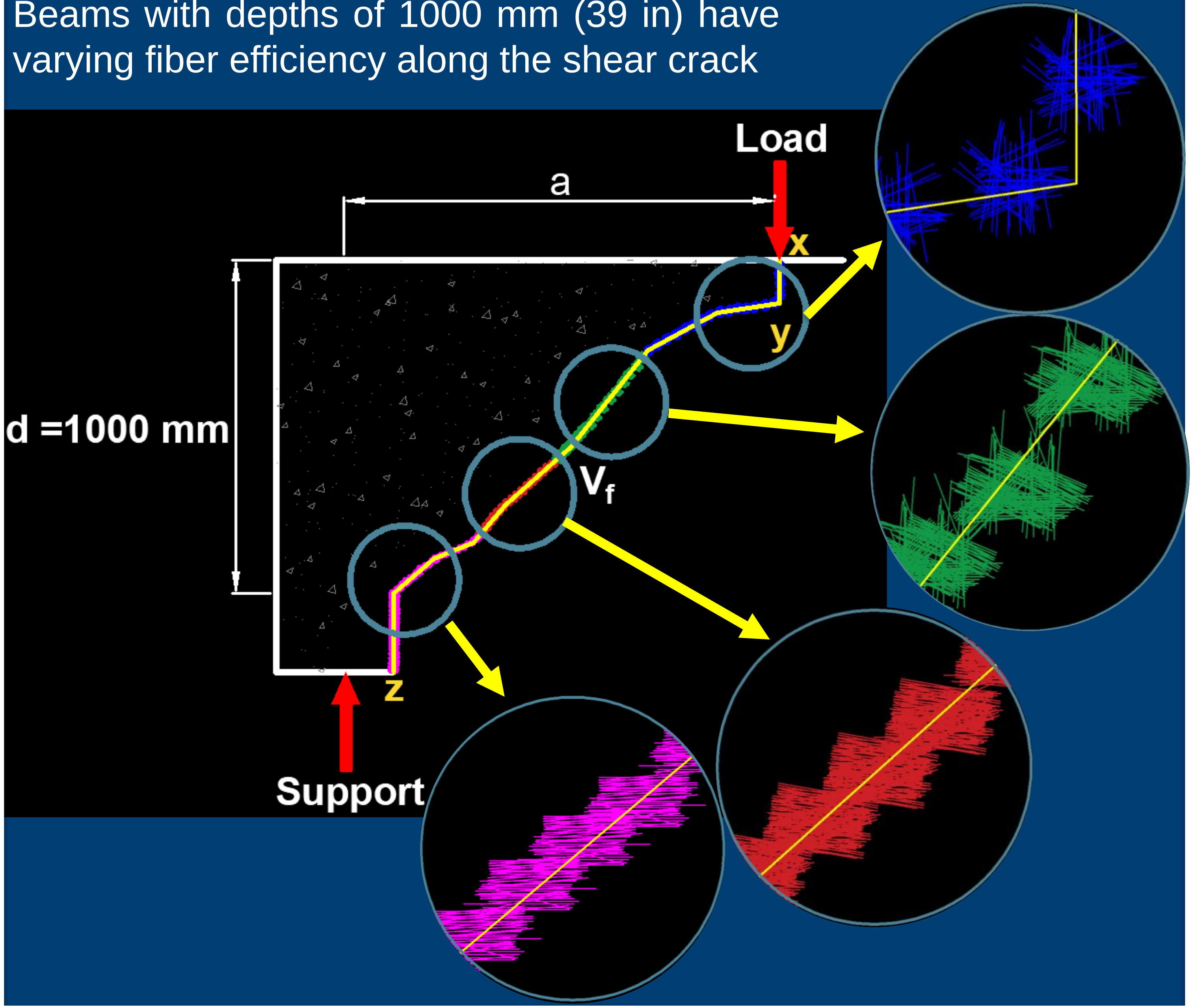

2 The fiber distribution effect has a higher impact on fiber orientation as the beams' depth increased

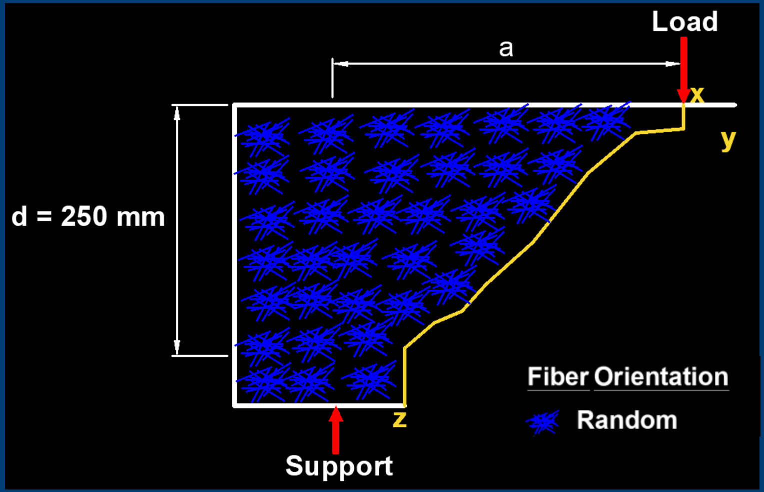

The fiber distribution effect cannot be noticed in beams with depths of 250 mm (10 in), therefore random orientation is expected.

1. The fibers that were decanted from the upper layers of UHPC modified the fiber orientation leading to the majority of the fibers in the lower layers to inclined at angles between 0° to 15° with respect to the X-Y plane.

2. As the layers of UHPC in the beams' depth increased, the fiber content was lower.

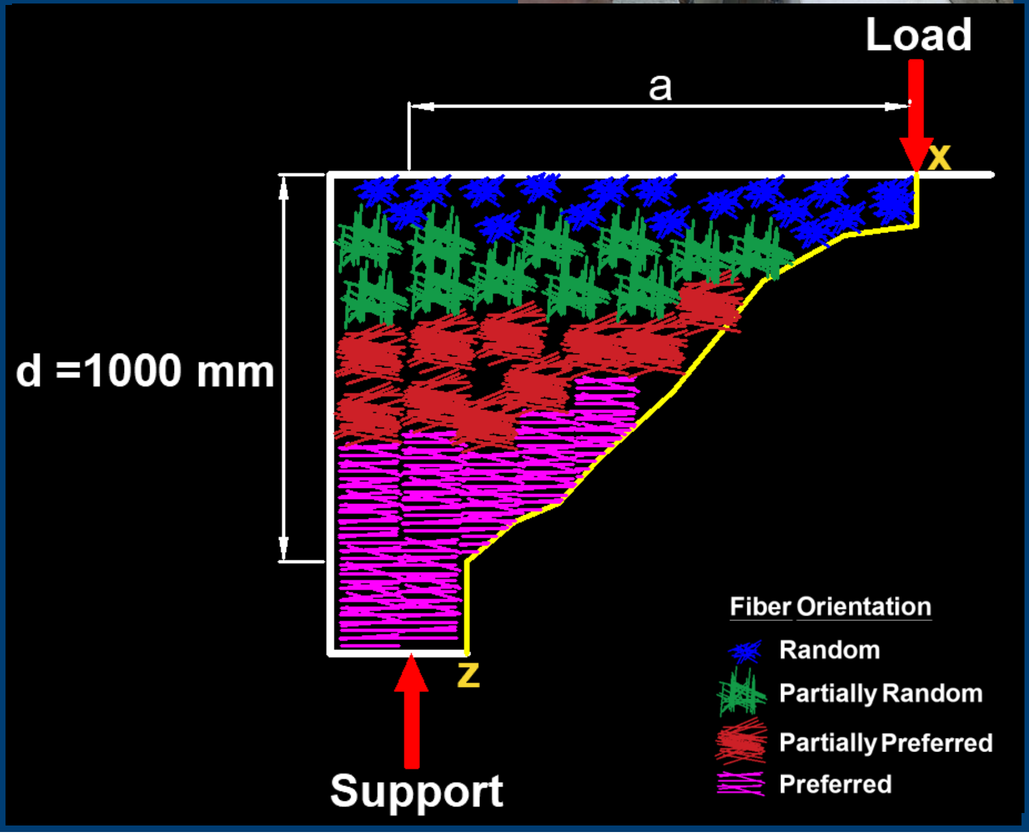

3 Considering the anisotropy of UHPC, is it reliable to use the tensile strength as the main beam shear predictor?

Longitudinal view

Cross-sectional view

Micro-CT scan

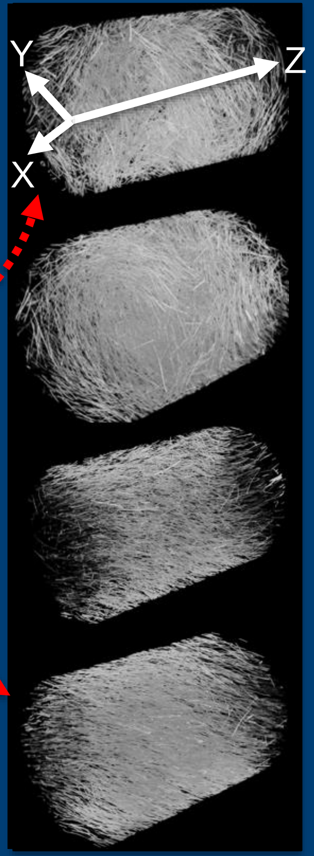

1. Fiber efficiency along the shear crack
2. Fiber distribution effect
3. Varying fiber orientation along the shear crack

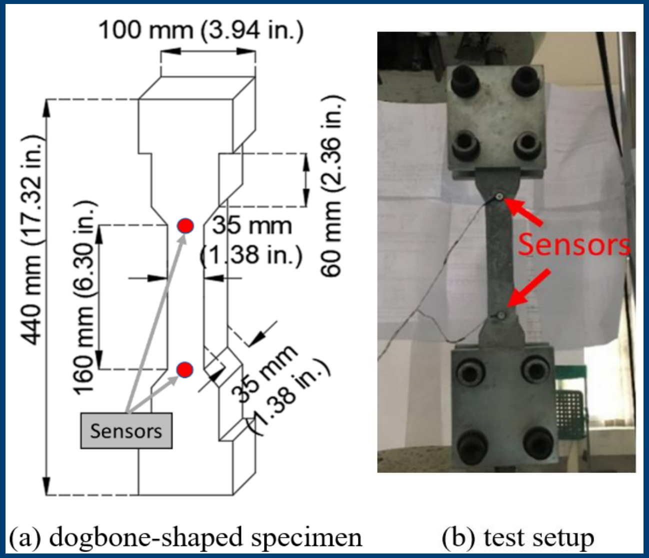

Direct tensile test (dogbone)

AASHTO T-397

Indirect tensile test (ASTM C1609)

3 Considering the anisotropy of UHPC, is it reliable to use the tensile strength as the main beam shear predictor?

Longitudinal view

Cross-sectional view

Micro-CT scan

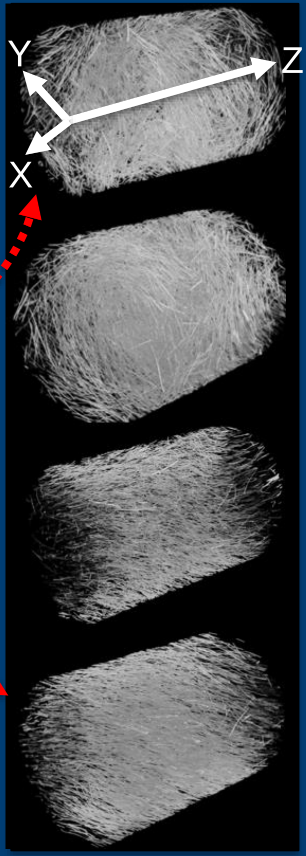

1. Fiber efficiency along the shear crack
2. Fiber distribution effect
3. Varying fiber orientation along the shear crack

Modified fiber factor (F) for UHPC

The original fiber factor was derived by Naaman (1972) using a probabilistic model.

$$F = F_{hybrid} = \sum_{i=1}^{n} \left(\frac{L_{f,i}}{D_{f,i}}\right) V_{f,i} d_{f,i}$$

$$v_b = v_{b,hybrid} = \sum_{i=1}^{n} 0.41 \tau_i F_i$$

The proposed shear strength equation was optimized with an evaluation database of 118 HS-HPFRC and UHPC non-prestressed beams and considers the size effect as ACI 318-19.

$$V_u = \sqrt{\frac{2}{1+\frac{d}{254}}} \left[2.25e\left(f'_c \rho_w \frac{d}{a}\right)^{0.57} + (1.80 v_b)^{1.3}\right] \left(\frac{b}{b_w}\right)^{0.35} \quad \text{(MPa)}$$

4 Evaluating the shear strength of UHPC I-shaped beams

Girder	f'c MPa [psi]	d (mm) [in]	ρ_w %	$V_{(Pred.)}$ MPa [psi]	V_{Test} MPa [psi]	V_{Test} / $V_{(Pred.)}$
B250-1.5F	127 [18]	250 [10]	7.4	8.6 [1247]	10.1 [1465]	1.17
B500-1.5F	140 [20]	500 [20]	7.4	7.3 [1059]	8.9 [1291]	1.21
B750-1.5F	140 [20]	750 [30]	9.0	7.5 [1088]	7.7 [1117]	1.01
B1000-1.5F	146 [21]	1000 [39]	10.6	7.7 [1177]	6.6 [957]	0.85
B750-0.75F	133 [19]	750 [30]	9.0	6.4 [928]	6.4 [928]	1.00

$$V_u = \sqrt{\frac{2}{1+\frac{d}{254}}}\left[2.25e\left(f'_c\rho_w\frac{d}{a}\right)^{0.57} + (1.80v_b)^{1.3}\right]\left(\frac{b}{b_w}\right)^{0.35} \quad \text{(MPa)}$$

Prestressed UHPC I-shaped beams

$$V_u = \sqrt{\frac{2}{1+\frac{d}{254}}}\left[2.25e\left(f'_c\rho_w\frac{d}{a}\right)^{0.57} + (1.80v_b)^{1.3}\right]\left(\frac{b}{b_w}\right)^{0.35} \boxed{+\,k_1\sigma_{cp}} \quad \text{(MPa)}$$

- k_1 = coefficient for the effect of the axial concrete stress on the shear capacity defined as 0.12 per DIN-EC2
- $\sigma_{cp} = N_{ed}/A_c < 0.20f'_c$

Girder	f'c (MPa) [ksi]	d (mm) [in]	ρ_w %	V_{cp} (MPa) [psi]	$V_{(Pred.)}$ (MPa) [psi]	V_{Test} (MPa) [psi]	V_{Test} / $V_{(Pred.)}$
UHPFRC-A-PC-NS [Baby et al. 2014]	203 [29]	305 [12]	4.5	1.4 [203]	16.9 [2451]	21.7 [3147]	1.3
UHPFRC-A(2)-PC-NS [Baby et al. 2014]	202 [29]	305 [12]	4.5	1.4 [203]	16.9 [2451]	21.7 [3147]	1.3
UHPFRC-B-PC-NS [Baby et al. 2014]	205 [30]	305 [12]	4.5	1.4 [203]	15.4 [2234]	25.6 [3713]	1.7
H-P1 [El-Helou et al. 2022]	137 [20]	813 [32]	7.4	2.6 [377]	12.5 [1813]	20.0 [2901]	1.6
J-P1 [El-Helou et al. 2022]	158 [23]	813 [32]	7.4	2.6 [377]	13.0 [1885]	20.4 [2959]	1.6
J-P1S [El-Helou et al. 2022]	152 [22]	821 [32]	5.5	2.0 [290]	11.2 [1624]	19.8 [2872]	1.8
H-P2 [El-Helou et al. 2022]	140 [20]	813 [32]	5.5	2.4 [348]	10.6 [1537]	18.1 [2625]	1.7

Thank you!

This study was sponsored in part by the National Science and Technology Council, Taiwan, under Grant No. 104-2628-E-006-002-MY3.

d = 250 mm d = 10 in | d = 500 mm d = 20 in | d = 750 mm d = 30 in | d = 1000 mm d = 39 in

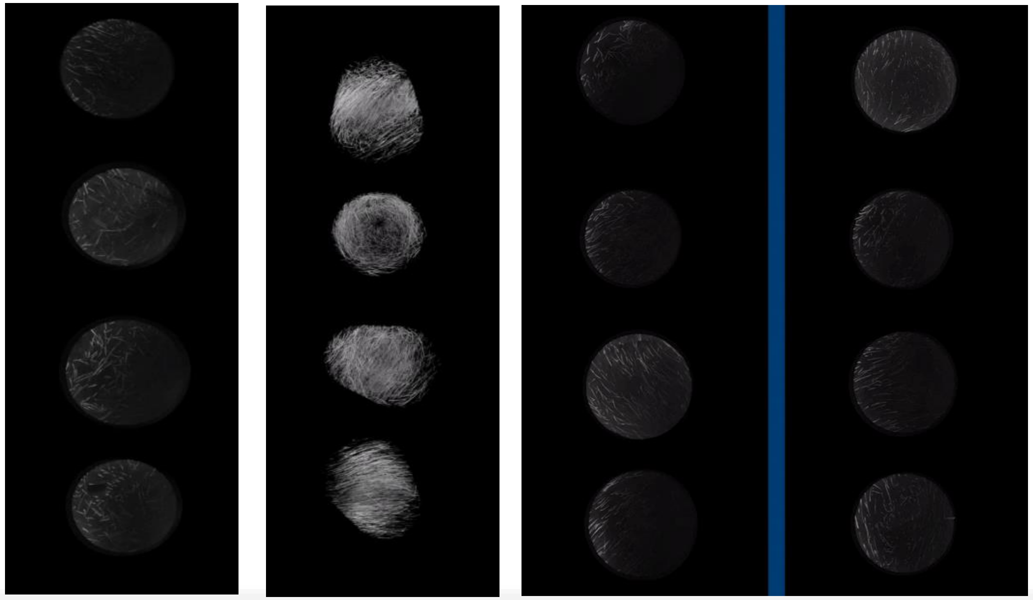

The authors acknowledge the support of the Laboratory Animal Center of the Faculty of Medicine at the National Cheng Kung University Center for the acquisition of the 3D micro-CT images.